Understanding the maximum dynamical heterogeneity during the unfreezing process in metallic glasses

B. Wang, L. J. Wang, W. H. Wang, H. Y. Bai, X. Q. Gao, M. X. Pan, and P. F. Guan

Citation: Journal of Applied Physics **121**, 175106 (2017); doi: 10.1063/1.4982914
View online: http://dx.doi.org/10.1063/1.4982914
View Table of Contents: http://aip.scitation.org/toc/jap/121/17
Published by the American Institute of Physics

Understanding the maximum dynamical heterogeneity during the unfreezing process in metallic glasses

B. Wang,[1,2,3] L. J. Wang,[3] W. H. Wang,[1,2] H. Y. Bai,[1,2] X. Q. Gao,[4] M. X. Pan,[1,2,a)] and P. F. Guan[3,a)]
[1]*Institute of Physics, Chinese Academy of Sciences, Beijing 100190, China*
[2]*School of Physical Sciences, University of Chinese Academy of Sciences, Beijing, China*
[3]*Beijing Computational Science Research Center, Beijing 100193, China*
[4]*Northwest Institute for Nonferrous Metal Research, Xian 710016, China*

(Received 7 March 2017; accepted 20 April 2017; published online 5 May 2017)

The dynamic behaviors displayed during the unfreezing process of metallic glasses are investigated using molecular dynamics simulations. The non-monotonic variation of dynamical heterogeneity as temperature increases can be understood microscopically by the flow unit perspective. This variation of dynamical heterogeneity exhibits a peak at the temperature $T_{\alpha_{2,max}}$ below the related α-relaxation temperature. Meanwhile, the $T_{\alpha_{2,max}}$ signaling the maximum dynamical heterogeneity is found to be the onset temperature at which the largest activated cluster starts to present the percolation property. Our results give hints to the understanding of low temperature relaxation and the related correlation with α relaxation in metallic glasses. *Published by AIP Publishing*. [http://dx.doi.org/10.1063/1.4982914]

I. INTRODUCTION

Liquid undergoes a glass transition by passing the formation of crystalline state and then transforms glasses. During this process, the liquid is too viscous to flow on available observation time scales.[1–3] This important phenomenon, which has been investigated by the glass research community for decades, is indeed a dynamic freezing process.[1,3,4] Plentiful critical temperatures are identified via both simulations and experiments,[5,6] at which the diversity and complexity of the relaxation dynamics are reflected and crossover events appear. These include the breakdown of the Stokes-Einstein relation,[2,5,7] the observing of dynamic heterogeneity,[2,8] the splitting of α and β relaxation,[1,9] and liquid-liquid transition,[10,11] amongst others. Many efforts have been devoted to revealing the detail and mechanism of the crossover events which occur in the freezing process of liquid from a high temperature flow state to the solid state.[12,13] However, less attention is paid to the dynamics of the reverse unfreezing process because the low temperature complex dynamics is fraught with difficulties caused by the off-equilibrium nature of glass[5,14] and the lack of relative effective approaches to study the process.[15]

With simple atomic packing and rotational degrees of freedom, metallic glass (MG) offers an effective model system to advance our understanding on some of the controversial issues surrounding liquid and of structural glass.[16,17] The dynamic mechanical spectroscopy (DMS) method is used to study the complex relaxation dynamics of MGs in both experimental and numerical studies[18] and some important intriguing issues have now been clarified, such as the relation between β relaxation and tensile plasticity and fragility.[19–21] However, so far the method has not been applied to the investigation of dynamical heterogeneity evolution, of which the microstructural features still lack direct proofs, although Li *et al*. have given some supposition of this during increasing temperature.[15] Recently, evidence has been supplied to verify the correlation between dynamical or spatial heterogeneity and relaxation dynamics.[22,23] Thus, it is possible to measure the dynamical heterogeneity evolution and study its rule using the DMS method during the unfreezing process.

In this paper, we employ the extensive molecular dynamics (MD) simulation method, which combines DMS and isoconfigurational ensemble, to study the dynamical heterogeneity evolution of MGs with increasing temperature. The calculated dynamical heterogeneity α_2, the non-Gaussian parameter, shows non-monotonic variation with increasing temperature and exhibits a peak at the temperature $T_{\alpha_{2,max}}$ which is below T_α, corresponding to the α-relaxation. The temperature dependent dynamical heterogeneity can be attributed to the activation of flow units during the unfreezing process. As the temperature increases, more and more flow units are activated and interconnect into larger clusters. The $T_{\alpha_{2,max}}$ signaling the maximum dynamical heterogeneity is found to be the onset temperature at which the largest activated cluster starts to present the percolation property. Our results help to clarify the atomic level features of the maximum dynamical heterogeneity during the unfreezing process and give hints to a relationship between α and low temperature relaxations in MGs.

II. MODEL AND METHODS

Molecular dynamics (MD) simulations were performed using the open source code-LAMMPS.[24] The prototype system $Zr_{50}Cu_{50}$ was selected as the subject of the study due to its superior glass-forming ability and simple constituents. The details of the embedded atom method (EAM) potential used can be inferred from Ref. 25. For initial sample

a)Authors to whom correspondence should be addressed. Electronic addresses: panmx@aphy.iphy.ac.cn and pguan@csrc.ac.cn

preparation, the system was first allowed to reach equilibrium at 1900 K under an external pressure of zero with the constant number, pressure, and temperature (NPT) ensemble for 10 ns. Following this, the sample was quenched to 50 K step by step at a rate of 10^{11} K/s with the NPT ensemble. The samples in Ref. 23 were also employed to ensure the validity of the results (for more details, see supplementary material). During the cooling process, the configurations of each sample at the temperatures of interest were collected for further dynamical mechanical spectroscopy. For all simulations, periodic boundary conditions were applied in three directions, the temperature is maintained by the Nosé-Hoover thermostat,[26] and the time step is 2 fs. In order to obtain the relaxation dynamics of glass, the extensive molecular dynamics (MD) simulation method was employed, which combines DMS and the isoconfigurational ensemble.[27] The details of the MD-DMS method can be found in the supplementary material.

III. RESULTS AND DISCUSSION

Figure 1(a) shows the temperature dependence of the loss modulus E'', based on the systematic MD-DMS simulations, which is analogous to the previous experimental and numerical results.[28,29] The curve presents the excess wing for the low temperature relaxation region and exhibits a peak at T_α that corresponds to α relaxation. This peak signals the model system transform from the glassy state to the supercooled liquid state, which means that the unfreezing of metallic glass can be achieved through cycle loading. This provides the opportunity to investigate the evolution of the dynamic properties of MGs with increasing temperature and thereby reveal insight into the atomic-level mechanism. To study the atomic dynamic behavior and the presence of dynamical heterogeneities, we calculated the self-part $G_s(r,t)$ of the van Hove correlation function, which is defined by

$$G_s(r,t) = \frac{1}{N}\left\langle \sum_{i=1}^{N} \delta\big(r + r_i(0) - r_i(t)\big) \right\rangle, \tag{1}$$

where $\delta(r)$ is the δ function and r is the distance traveled by a particle in the time t.[8,30,31] The physical meaning of $G_s(r,t)$ is the probability of finding a particle in the distance of "r" at some other time "t" and the volume integral of it is a conserved quantity and equals unity. Hence, $4\pi r^2 G_s(r,t)$ reflects the probability distribution density of the displacement within time interval t and has the same physical meaning of $p(u)$, which has been introduced in previous studies.[23,27,32] Obviously, the shape of $4\pi r^2 G_s(r,t)$ reflecting the dynamic behavior is dependent on the observation time[33] or interval time t. Since we are trying to understand the dynamic behaviors during the unfreezing process by cycle loading, we set the interval time t as $t_p = 100$ ps, the period of cycle loading, for all investigated temperatures to avoid the influence of the observation time. The calculated $4\pi r^2 G_s(r, t = 100\,\text{ps})$ for different temperatures is shown in Figure 1(b). As expected, this probability distribution is found to broaden with increasing temperature, which is consistent with previous studies.[32] If there is no local atomic rearrangement, $G_s(r,t)$ should have a standard Gaussian form with

$$G_s^g(r,t) = \left[3/2\pi\langle r^2(t)\rangle\right]^{\frac{3}{2}} \exp\left[-3r^2/2\langle r^2(t)\rangle\right], \tag{2}$$

according to the thermal vibration effect. Here, we assume that the atomic displacements within the time interval $t = 100$ ps at low temperatures are mainly caused by thermal vibration and $4\pi r^2 G_s^g(r, t = 100\,\text{ps})$ should have the same mode as the calculated $4\pi r^2 G_s(r, t = 100\,\text{ps})$. The curves of $4\pi r^2 G_s(r, t = 100\,\text{ps})$ and $4\pi r^2 G_s^g(r, t = 100\,\text{ps})$ at 750 K are shown in the inset of Figure 1(b). Obviously, the difference

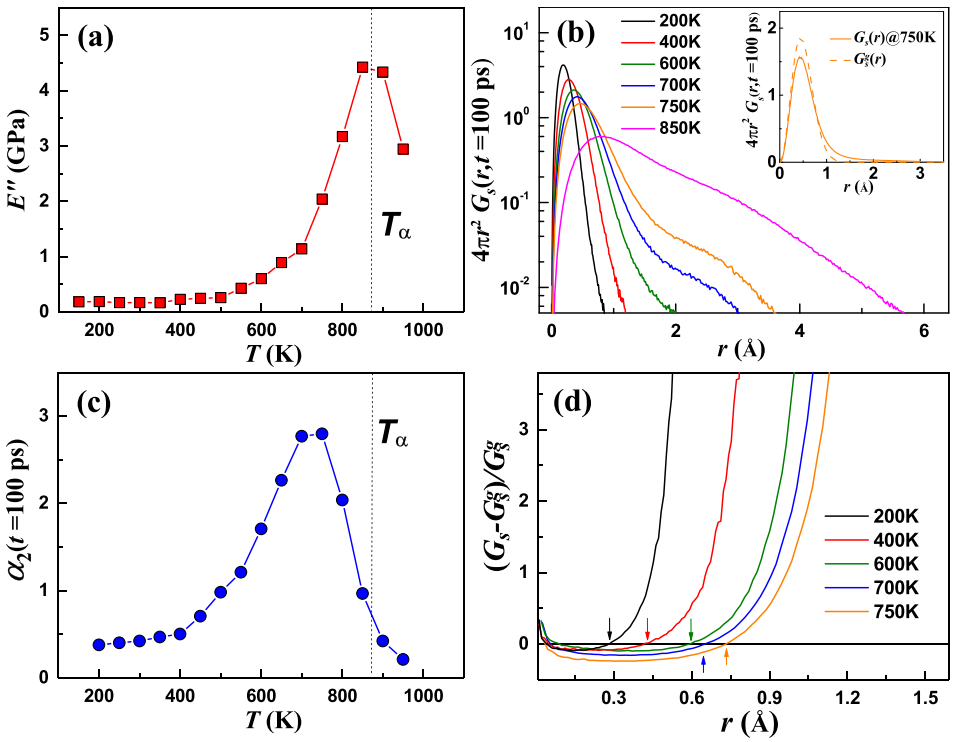

FIG. 1. (a) Temperature dependence of loss modulus E''. (b) The quantity $4\pi r^2 G_s(r)$ for all particles at different temperatures, where $G_s(r)$ is the von Hove correlation function and $G_s(r)$ has a Gaussian form if the dynamical heterogeneity does not exist. The inset of the figure represents the difference between the actual quantity $4\pi r^2 G_s(r)$ and quantity $4\pi r^2 G_s^g(r)$, where $G_s^g(r)$ represents the standard Gaussian form. (c) The Non-Gaussian parameter α_2 versus temperature T. (d) The $(G_s(r)\text{-}G_s^g(r))/G_s^g(r)$ versus displacement r at different temperatures. The cutoff distances were determined by the deviation from the Gaussian form, in other words, at the point where the $(G_s(r)\text{-}G_s^g(r))/G_s^g(r)$ becomes positive and increases sharply.

between $4\pi r^2 G_s^g(r, t = 100\,\text{ps})$ and the calculated $4\pi r^2 G_s(r, t = 100\,\text{ps})$ highlights the non-Gaussian behavior of $G_s(r, t = 100\,\text{ps})$. This confirms the theory of local atomic rearrangements and dynamical heterogeneity in MGs during sinusoidal strain driving at low temperatures. This is consistent with the concept of structural and dynamical heterogeneities in MGs and agrees with the structural model in which the MGs consist of elastic regions (or solid-like regions) and inelastic regions (or liquid-like regions).[34,35] The liquid-like regions can easily be activated during the loading process and are responsible for the viscoelastic flow of glass.[34,36] To quantify the dynamical heterogeneity in the sinusoidal strain driven system, the non-Gaussian parameter

$$\alpha_2(t = t_p) = 3\langle r^4(t)\rangle / 5\langle r^2(t)\rangle^2 - 1, \tag{3}$$

which is a departure from standard Gaussian form, was used for this study, with the larger value of α_2 reflecting the more heterogeneous dynamics of the glass.[8] The computed $\alpha_2(t = 100\,\text{ps})$ in the temperature range of 200–950 K is shown in Figure 1(c). It shows that the dynamical heterogeneity appears to vary non-monotonically with increasing temperature and presents a peak at $T_{\alpha_{2,max}}$, which is below T_α. It is consistent with the recent experimental work in which the non-monotonic evolution of dynamical heterogeneity was found with increasing temperature,[16] but the precise atomic level features remain unclear. We also measured the temperature dependence of $\alpha_2(t = 100\,\text{ps})$ for the various samples employed in Ref. 23 and all curves of the samples exhibit a peak at a temperature below its T_α (see supplementary material). It confirms that (i) the dynamic response of MGs corresponding to sinusoidal strain loading becomes more heterogeneous with increasing temperature; (ii) a maximum value of $\alpha_2(t = 100\,\text{ps})$ can be observed before the system transforms from the glassy state to the supercooled liquid state; and (iii) $\alpha_2(t = 100\ \text{ps})$ decreases to zero at very high temperatures. This is evidence that there is coupling between dynamical heterogeneity and the relaxation behavior at low temperatures, but decoupling as the temperature gets close to T_α.

To understand the monotonic increase of $\alpha_2(t = 100\,\text{ps})$ in the low temperature regime and what happens at the temperature $T_{\alpha_{2,max}}$, we selected the atoms which contribute to the value of $\alpha_2(t = 100\,\text{ps})$. First, we compared the calculated $G_s(r, t = 100\,\text{ps})$ with the distribution $G_s^g(r, t = 100\,\text{ps})$ that is obtained from the Gaussian approximation. Figure 1(d) shows the $[G_s(r,t) - G_s^g(r,t)]/G_s^g(r,t)$ with $t = 100$ ps for various temperatures. The relative difference between G_s^g and G_s is weak for small and intermediate values of r, but strong for larger r, which means that G_s^g underestimates G_s significantly for larger r. It is evidence that a significant number of atoms move farther than expected from the Gaussian approximation and the heterogeneity or relaxation is mainly contributed to by fast dynamic atoms, which is consistent with previous studies.[27] Therefore, we can define a cutoff distance r_{cut} to select the "fast dynamic atoms" as atoms that have moved farther than a distance r_{cut} within a time $t_p = 100$ ps. Here, we define r_{cut} as the larger of the two values of r for which $G_s^g(r_{cut}) = G_s(r_{cut})$, shown by the arrow point in Figure 1(d); i.e., r_{cut} is the value of r at which the difference between $G_s^g(r_{cut})$ and $G_s(r_{cut})$ starts to become positive and very large. The atoms can then be divided into two parts at each temperature: the slow atoms belonging to the elastic matrix and the fast atoms that mainly contribute to the dynamic relaxation. The fast atoms can be viewed as "flow units," considering that flow units are any available and thermally or mechanically activated localized rearrangements.[34,36,37] The calculated fractions of average numbers of selected fast atoms are shown in Figure 2(a) (red histogram). The fraction of selected atoms increases as temperature increases and this suggests that more and more flow units are activated and then that enhances the dynamic heterogeneity. At $T = T_{\alpha_{2,max}} = 750$ K, the fraction of selected fast atoms approaches 25% (red histogram in Figure 2(a)), and the value agrees well with the fraction of frozen liquid-like atoms, 24.3%, in the theory of the glass transition for metallic glass.[38,39] In essence, the dynamical heterogeneity results from the frozen liquid-like atoms below T_g. When nearly all the frozen liquid-like atoms are activated, the dynamical heterogeneity of the system achieves its maximum. Thus, the crossover of α_2 at $T_{\alpha_{2,max}}$ (see Figure 1(c)) may suggest a dramatical change of relaxation behavior corresponding to the onset temperature $T_{\alpha_{2,max}}$.

To investigate the evolution of the relaxation behavior with increasing temperature, we analyzed the microscopic features of selected fast atoms (or flow units) for $T < T_{\alpha_{2,max}}$. The spatial correlation between selected atoms is shown in Figure 2(b), where we compare (cf. inset) $g_s(r)$ and $g_{all}(r)$, the radial distribution functions for the fast atoms and for the bulk, respectively. We find that at the first peak, at lower temperatures the fast atoms are more strongly correlated than the bulk. This is demonstrated more clearly by computing the

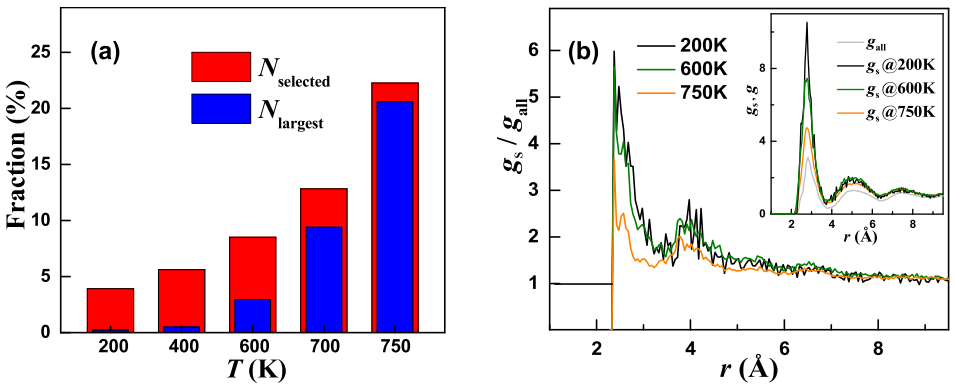

FIG. 2. (a) The red and blue histograms represent the fractions of average numbers of selected fast dynamics atoms (or flow unit atoms) and the largest cluster atoms formed by "flow units" at different temperatures, respectively. (b) Inset: radial distribution function $g_s(r)$ and $g_{all}(r)$ for the fast dynamic atoms and bulk atoms. Main figure: Ratio between $g_s(r)$ and $g_{all}(r)$ for different temperatures. 750 K is the temperature at which the dynamical heterogeneity is the most obvious.

ratio g_s/g_{all}, which is shown in Figure 2(b) for three different temperatures. From this figure, we can infer that the relatively strong correlation between the fast atoms at 200 K suggests that the flow units tend to form clusters and the size of a cluster is on the order of 5 A. This can be confirmed by the motif of these atoms (see Figure 3(a)) and the atomic fraction of the largest cluster (see Figure 2(a), blue histogram). As shown in Figure 3(a), the clusters constructed by flow units disperse homogenously in the system. As the temperature increases, the difference between the g_s and g_{all} becomes weaker and the atomic fraction of the largest cluster becomes bigger. It suggests that more and more flow units are activated and form bigger clusters by interconnecting, which is supported by the spatial distribution of selected atoms in Figures 3(b) and 3(c). Finally, nearly all the flow units involve in the largest cluster and the largest cluster, the red cluster in Figure 3(d), passes through the whole system at the temperature $T = T_{\alpha_{2,max}} = 750$ K. Similar results were also obtained when the various samples from Ref. 23 were studied. It implies that the system at $T_{\alpha_{2,max}}$ behaving with maximum dynamical heterogeneity starts to show the percolation property of the largest activated cluster. The temperature $T_{\alpha_{2,max}}$ roughly corresponds to the temperature at which α relaxation begins in Figure 1(a), and we can speculate that the flow units tend to interconnect with each other and form extended cooperative flowing regions at this temperature. Therefore, the α-process begins to contribute to the relaxation dynamics. This is consistent with the result that nearly all the frozen liquid-like atoms are activated at $T_{\alpha_{2,max}}$, which implies that glass transition or α relaxation starts to occur through the percolation transition of liquid-like states, as predicted by Cohen and Grest.[40] It indicates that we could tune the properties of metallic glasses effectively just above $T_{\alpha_{2,max}}$, but not necessarily above the glass transition temperature T_g. Furthermore, the consequences may suggest that the low temperature relaxation can act as a precursor of α relaxation and the relation between α and low temperature relaxation will be clarified in the further.

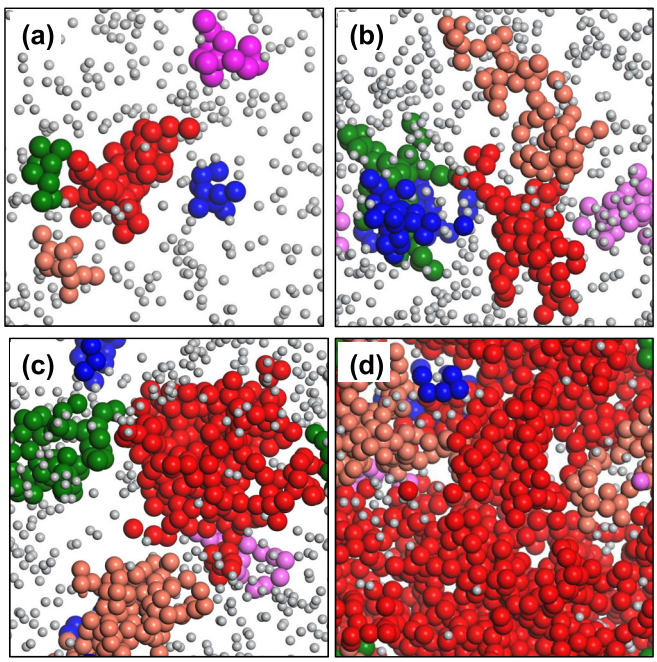

FIG. 3. (a)–(d) Snapshots of the configuration of flow units at different temperatures of 200 K, 600 K, 700 K, and 750 K, respectively, in which the top five largest clusters are labeled as red, pink, green, rose red, and blue colors in order of size and the gray atoms represent ones in small clusters. 750 K is the temperature at which the dynamical heterogeneity is the most obvious.

IV. CONCLUSIONS

In summary, the non-monotonic evolution of dynamical heterogeneity was found during the unfreezing process and the maximum of dynamical heterogeneity appears at a temperature below T_α. The flow unit perspective was applied to account for the phenomenon microscopically. As temperature increases, more and more flow units are activated and tend to interconnect into larger clusters during this unfreezing process, and then at the temperature $T_{\alpha_{2,max}}$ the largest cluster starts to show the percolation property. Our results also provide new insights into the correlation between α relaxation and low temperature relaxation.

SUPPLEMENTARY MATERIAL

See supplementary material for the MD-DMS method and details about samples employed in Ref. 23. It also provides the dynamical heterogeneity evolution of these samples to ensure the validity of the results in the manuscript.

ACKNOWLEDGMENTS

Insightful discussions with K. L. Ngai, B. S. Shang, P. Luo, Y. C. Wu, L. J. Wang, and S. Zhang are highly acknowledged. We also thank D. W. Ding, D. Q. Zhao, and B. B. Wang for helpful discussions. The financial support of the NSF of China (Grant No. 51571011), the NSAF of China (Grant No. U1530401), and the MOST 973 Program (No. 2015CB856800) is acknowledged. B.W., W.H.W., H.Y.B., and M.X.P. are also supported by the NSF of China (Grant Nos. 51571209, 51461165101, and 51601150).

[1]P. G. Debenedetti and F. H. Stillinger, Nature **410**, 259 (2001).
[2]M. D. Ediger and P. Harrowell, J. Chem. Phys. **137**, 080901 (2012).
[3]C. A. Angell, Curr. Opin. Solid State Mater. Sci. **1**, 578 (1996).
[4]G. Biroli and J. P. Garrahan, J. Chem. Phys. **138**, 12A301 (2013).
[5]K. L. Ngai, *Relaxation and Diffusion in Complex Systems* (Springer Science & Business Media, 2011).
[6]P. G. Wolynes and V. Lubchenko, preprint arXiv:cond-mat/0607349.
[7]X. J. Han, J. G. Li, and H. R. Schober, J. Chem. Phys. **144**, 124505 (2016).
[8]W. Kob, C. Donati, S. J. Plimpton, P. H. Poole, and S. C. Glotzer, Phys. Rev. Lett. **79**, 2827 (1997).
[9]J. Hachenberg, D. Bedorf, K. Samwer, R. Richert, A. Kahl, M. D. Demetriou, and W. L. Johnson, Appl. Phys. Lett. **92**, 131911 (2008).
[10]S. Sastry and C. A. Angell, Nat. Mater. **2**, 739 (2003).
[11]J. C. Palmer, F. Martelli, Y. Liu, R. Car, A. Z. Panagiotopoulos, and P. G. Debenedetti, Nature **510**, 385 (2014).
[12]J. Dyre, Rev. Mod. Phys. **78**, 953 (2006).
[13]S. Hudson and H. C. Andersen, J. Chem. Phys. **69**, 2323 (1978).
[14]C. A. Angell, K. L. Ngai, G. B. McKenna, P. F. McMillan, and S. W. Martin, J. Appl. Phys. **88**, 3113 (2000).
[15]Y. Z. Li, L. Z. Zhao, C. Wang, Z. Lu, H. Y. Bai, and W. H. Wang, J. Chem. Phys. **143**, 041104 (2015).
[16]Y. Q. Cheng and E. Ma, Prog. Mater. Sci. **56**, 379 (2011).
[17]M. Ashby and A. Greer, Scr. Mater. **54**, 321 (2006).
[18]H. B. Yu, W. H. Wang, H. Y. Bai, and K. Samwer, Nat. Sci. Rev. **1**, 429 (2014).

[19]K. L. Ngai, L. M. Wang, R. Liu, and W. H. Wang, J. Chem. Phys. **140**, 044511 (2014).
[20]H. B. Yu, X. Shen, Z. Wang, L. Gu, W. H. Wang, and H. Y. Bai, Phys. Rev. Lett. **108**, 015504 (2012).
[21]H. B. Yu, Z. Wang, W. H. Wang, and H. Y. Bai, J. Non-Cryst. Solids **358**, 869 (2012).
[22]F. Zhu, H. K. Nguyen, S. X. Song, D. P. Aji, A. Hirata, H. Wang, K. Nakajima, and M. W. Chen, Nat. Commun. **7**, 11516 (2016).
[23]B. Wang, B. S. Shang, X. Q. Gao, W. H. Wang, H. Y. Bai, M. X. Pan, and P. F. Guan, J. Phys. Chem. Lett. **7**, 4945 (2016).
[24]S. Plimpton, J. Comput. Phys. **117**, 1 (1995).
[25]Y. Q. Cheng, H. W. Sheng, and E. Ma, Phys. Rev. B **78**, 014207 (2008).
[26]G. J. Martyna, M. L. Klein, and M. Tuckerman, J. Chem. Phys. **97**, 2635 (1992).
[27]H.-B. Yu and K. Samwer, Phys. Rev. B **90**, 144201 (2014).
[28]Z. G. Zhu, Y. Z. Li, Z. Wang, X. Q. Gao, P. Wen, H. Y. Bai, K. L. Ngai, and W. H. Wang, J. Chem. Phys. **141**, 084506 (2014).
[29]Y. Cohen, S. Karmakar, I. Procaccia, and K. Samwer, Europhys. Lett. **100**, 36003 (2012).
[30]J.-P. Hansen and I. R. McDonald, *Theory of Simple Liquid* (Academic, London, 1986).
[31]S. Sastry, P. G. Debenedetti, and F. H. Stillinger, Nature **393**, 554 (1998).
[32]H. B. Yu, R. Richert, R. Maass, and K. Samwer, Nat. Commun. **6**, 7179 (2015).
[33]X. Q. Gao, W. H. Wang, and H. Y. Bai, J. Mater. Sci. Technol. **30**, 546 (2014).
[34]Z. Lu, W. Jiao, W. H. Wang, and H. Y. Bai, Phys. Rev. Lett. **113**, 045501 (2014).
[35]P. Y. Huang, S. Kurasch, J. S. Alden *et al.*, Science **342**, 224 (2013).
[36]Z. Wang, B. A. Sun, H. Y. Bai, and W. H. Wang, Nat. Commun. **5**, 5823 (2014).
[37]Y. C. Hu, P. F. Guan, M. Z. Li, C. T. Liu, Y. Yang, H. Y. Bai, and W. H. Wang, Phys. Rev. B **93**, 214202 (2016).
[38]T. Egami, S. J. Poon, Z. Zhang, and V. Keppens, Phys. Rev. B **76**, 024203 (2007).
[39]W. Dmowski, T. Iwashita, C. P. Chuang, J. Almer, and T. Egami, Phys. Rev. Lett. **105**, 205502 (2010).
[40]M. H. Cohen and G. S. Grest, Phys. Rev. B **20**, 1077 (1979).